HHS Public Access

Author manuscript

J Am Chem Soc. Author manuscript; available in PMC 2024 October 02.

Published in final edited form as:

J Am Chem Soc. 2020 March 11; 142(10): 4565–4569. doi:10.1021/jacs.9b13997.

Single-Chain Nanoparticle Delivers a Partner Enzyme for Concurrent and Tandem Catalysis in Cells

Junfeng Chen[†], **Ke Li**[†], **Jiseon "Lucy" Shon**[†], **Steven C. Zimmerman**[*,†,‡]

[†]Department of Chemistry, University of Illinois, Urbana, Illinois 61801, United States.

[‡]Center for Biophysics and Quantitative Biology, University of Illinois, Urbana, Illinois 61801, United States.

Abstract

Combining synthetic chemistry and biocatalysis is a promising but underexplored approach to intracellular catalysis. We report a strategy to co-deliver a single-chain nanoparticle (SCNP) catalyst and an exogenous enzyme into cells for performing bioorthogonal reactions. The nanoparticle and enzyme reside in endosomes, creating engineered artificial organelles that manufacture organic compounds intracellularly. This system operates in both concurrent and tandem reaction modes to generate fluorophores or bioactive agents. The combination of SCNP and enzymatic catalysts provides a versatile tool for intracellular organic synthesis with applications in chemical biology.

Graphical Abstract

[*]**Corresponding Author:** sczimmer@illinois.edu.

Supporting Information.

The Supporting Information is available free of charge on the ACS Publications website at DOI:

General experimental procedures and detailed synthetic procedures and characterization data for small molecules and polymers, and additional kinetic data along with details of the computational methods (PDF)

The authors declare no competing financial interest.

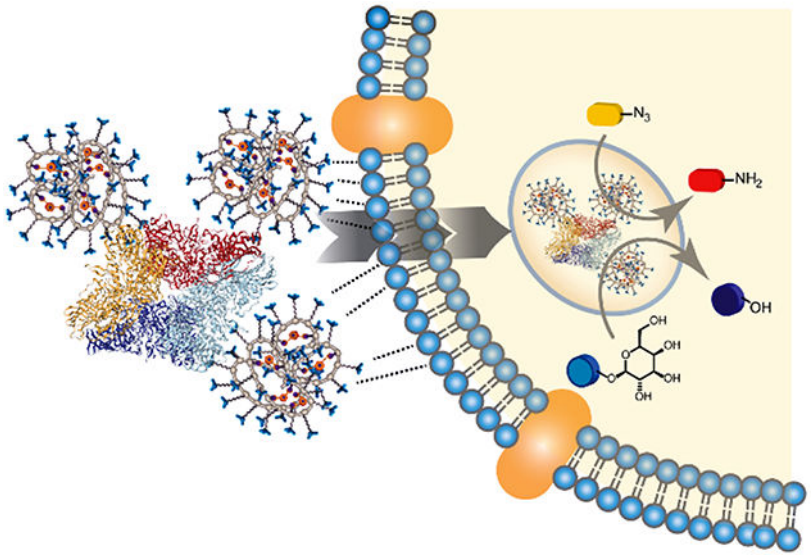

Developing robust and high yielding synthetic organic reactions inside living cells represents a new and important challenge. The ability to generate organic compounds in situ has potential applications in both chemical biology and medicinal chemistry.[1–3] To access more complicated targets, efforts have been made to conduct two or more reactions intracellularly, but it is critical to expand beyond the limited examples reported to date.[4,5] The recent success in combining synthetic reactions and biocatalysis,[6,7] inspired us to explore the potential of conducting such dual catalysis inside cells. However, several challenges remain. For example, chemical catalysts are typically less efficient compared to enzymes especially with the low substrate concentrations in cells. Additionally, enzymes and chemical catalysts are not always taken up by cells, requiring complicated delivery methods.[8]

To increase the compatibility between chemical and biocatalysts, efforts have focused on developing biofriendly metallocatalysts. Synthetic polymers, nanoparticles, metal-organic cages, engineered proteins, and micelles were all reported to encapsulate transition metal catalysts that perform in aqueous or even biological environments.[9–13] We developed crosslinked copper-containing SCNPs as enzyme-like catalysts to perform high efficiency alkyneazide cycloaddition (CuAAC) reactions in water.[14–20] In addition, some SCNPs penetrate cell membranes, performing reactions inside living cells.[21–23] Herein we report a new SCNP catalyst capable of delivering an exogenous enzyme to cells and performing both concurrent and tandem catalysis.

We chose to develop SCNP containing the tris(bipyridine)ruthenium ($Ru(bpy)_3$) complex to photo-catalytically reduce azide into amino groups. This reaction and its biocompatibility were studied independently by the Liu and Winssinger groups.[24,25] This particular catalyst is robust, but has poor cell permeability and a low reaction rate under highly diluted conditions, making it an ideal candidate for the SCNP approach.[26,27]

The preparation of the $Ru(bpy)_3$-containing SCNP (**RuSCNP**) followed our reported “folding and crosslinking” strategy in water to suppress intermolecular crosslinking.[15] Thus,

water-soluble polymer **P1** was intramolecularly crosslinked with $Ru(bpy)_3$ diyne **1** using the CuAAC reaction. **RuSCNP** was characterized by transmission electron microscopy (TEM), diffusion ordered spectroscopy (DOSY) and NMR relaxation times (Figure S1). The diameter of **RuSCNP** was calculated to be around 7 nm by DOSY.

The catalytic activity of **RuSCNP** was first compared with **1** and $Ru(bpy)_3$ in PBS buffer. To test the reaction at micromolar concentrations typically used in biological studies, we used fluorogenic substrate **2**.[28] Reduction of the azido groups in **2** produces highly fluorescent rhodamine110 (**3**), and the reaction conversion can readily be monitored by the fluorescence increase. The reactions were conducted by irradiating the solution at 470 nm with sodium ascorbate (NaAsc) as the reducing agent. As shown in Figure 2a, all the reactions were performed at [Ru] = 1 μM for comparison. Both **1** and $Ru(bpy)_3$ exhibit comparatively weak activity at this low concentration. In contrast, **RuSCNP** performed the azide reduction with significantly higher efficiency, nearly full conversion occurring within 10 min irradiation. Control experiments without catalyst, irradiation, or NaAsc showed no reaction (Figure S2), results that are consistent with **RuSCNP** binding hydrophobic **2** in proximity to the internal $Ru(bpy)_3$ catalytic centers.

The intracellular azide reduction activity of **RuSCNP** was studied using HeLa cells (Figure 2b) whose uptake ability was studied using Lysotracker. The colocalization of fluorescence from Lysotracker and the $Ru(bpy)_3$ units showed the nanoparticle to enter through endocytosis (Figure S3). For catalytic runs, the cells were incubated with **RuSCNP**, washed extensively to remove extracellular catalyst, **2** was added, the cells irradiated at 470 nm, and confocal microscopy performed. As shown in Figure 2b, strong green fluorescence from **3** was observed largely colocalized with the **RuSCNP**, but also dispersed throughout the cytosol. This observation is consistent with azide reduction occurring largely within the endosomes.

Many examples of intracellular catalysis use small molecule-based catalysts that rapidly equilibrate between intra- and extra-cellular spaces, making it difficult to definitively establish an intracellular reaction.[1,29] In this work, an intracellular reaction is supported by the following observations. First, almost no **RuSCNP** was found to diffuse out when washing the cells with PBS buffer (Figure S6a), presumably because the polymeric nanoparticles stably reside within the endosomes of cells. Second, without the addition of NaAsc, the **RuSCNP** must use endogenous reductants within the cell (Figure S6b). No suitable reductant is present in the extracellular PBS buffer. Finally, the fluorescence of **3** initially showed significant overlap with the **RuSCNP** emission suggesting the production of **3** by the nanoparticles within endosomes and its subsequent migration to the cytosol.

Related cationic and amphiphilic SCNPs were shown to bind protein surfaces reversibly through a combination of electrostatic and hydrophobic interactions.[15] Such complexation suggested that **RuSCNP** might bind and deliver enzymes across cell membranes,[30] thereby allowing SCNP-enzyme concurrent and tandem catalysis (Figure 4a). β-Galactosidase (βGal), which catalyzes the hydrolysis of β-galactosides, was chosen as a model exogenous enzyme. Coumarin derivative **4** was used as the fluorogenic substrate for βGal.[31] The ability to perform concurrent tandem catalysis was first examined in HeLa cell lysate containing

[**RuSCNP**] = 200 nM, [βGal] = 20 nM, [**2**] = 20 μM, [**4**] = 100 μM and [NaAsc] = 2 mM. After 10 min irradiation at 470 nm, both reactions reached a high level of conversion: 84% for azido substrate **2** and more than 95% for the enzymatic reaction of **4**.

Having established the efficiency and bioorthogonality of the chemical and enzymatic reactions, the ability of **RuSCNP** to bind βGal was tested. By measuring the fluorescence anisotropy, the polarization of βGalF was found to increase with increasing [**RuSCNP**]. As shown in Figure 3a, the polarization of βGalF exhibited a sharp increase with the addition of 2.5 equivalents of **RuSCNP**, and a plateau at 10 equivalents. This observation suggests βGal might bind 2–3 of **RuSCNP** relatively tightly and offer weaker binding towards additional **RuSCNP**. The apparent K_d was calculated to be ca. 31 nM which is significantly lower than that for the related nanoparticle-protein complex (Cu-SCNP and BSA) previously reported.[15] The stronger binding here arises from two major differences. First, the molecular weight of βGal (464 kDa) is much larger than BSA (66 kDa), **RuSCNP** (40 kDa) and the Cu-SCNP (28 kDa), leading to more multivalent binding contacts. Second, the $Ru(bpy)_3$ complexes in **RuSCNP** appear to contribute significantly to the binding. Thus, saturation transfer difference (STD) spectroscopy showed the most intense contacts between the bipyridine units and the enzyme (Figure 3b).

To test whether the complex formed between **RuSCNP** and βGal facilitates the enzyme's uptake in living cells, HeLa cells were incubated with fluorescein labelled βGal (βGalF) alone or with either **RuSCNP** or $Ru(bpy)_3$. As shown in Figure S7, **RuSCNP** successfully delivered βGalF to the cells and tended to reside within endosomes, whereas almost no protein and Ru uptake was observed in the other two experiments lacking the nanoparticle.

The SCNP-enzyme concurrent intracellular catalysis was examined using substrates **2** and **4**. Again, HeLa cells were incubated with a 10:1 ratio of **RuSCNP** to βGal, washed extensively with buffer, substrates **2** and **4** added, and irradiated at 470 nm. As measured by confocal microscopy (Figure 4b) and flow-cytometry (Figure S7), both SCNP catalyzed and enzymatic reactions were successfully performed with fluorescence increasing over time, whereas the analogous experiments conducted with $Ru(bpy)_3$ and βGal resulted in almost no fluorescence (Figure S8). The cells were lysed after the reactions, and the lysate was analyzed by fluorimetry and HPLC (see supporting information for details). The conversion of **2** to **3** was 83% measured by fluorimetry and more than 90% by HPLC analysis. ICP analysis performed on the cell lysate gave the [Ru] to be 1.4 μM. Based on [**3**] determined by HPLC, the turnover number (TON) was estimated to be 26, indicating that the reaction is catalytic. For the enzymatic reaction, both fluorimeter and HPLC measurements suggested greater than 90% conversion of **4** to **5**.

The dual catalysis described above suggests that endosomes containing **RuSCNP** and βGal may serve as artificial organelles to perform intracellular synthesis. As proof of concept, a dual drug production experiment was performed. Doxorubicin derivative **6** and galactose-masked combretastatin A4 **7** were chosen as the prodrugs,[32,33] both producing anticancer agents after intracellular activation. HeLa cells were incubated with both prodrugs following the protocols above. After 5 min irradiation at 470 nm, cells containing **RuSCNP**, Gal, **6** and **7** exhibited significant cell death (Figure 4c). With only one prodrug, cell death was also

observed, but to a lower extent. These results suggest the SCNP-enzyme system functions like an intracellular factory to produce bio-active agents.

Finally, we explored the possibility of building a tandem reaction based on **RuSCNP** and βGal. The hydroxyl groups of **4** were covalently masked with an azido phenyl carbonate unit **8**, which prevents the βGal mediated cleavage (Figure 4d). Because of nonspecific intracellular hydrolysis,[34] two of four hydroxyl groups were randomly masked to minimize background reaction. During the tandem catalysis, both two azido caging groups need to be reduced and cleaved from the galactose, and βGal subsequently hydrolyzes **4** to generate fluorescent product **5**. The reaction was performed in HeLa cell lysate with [**RuSCNP**] = 200 nM, [βGal] = 20 nM, [**8**] = 20 μM and [NaAsc] = 2 mM, and about 20% conversion was reached after 10 min irradiation. Unfortunately, in live HeLa cells, almost no increase in fluorescence was observed, possibly a result of poor cell permeability of **8** (MW ca. 700 Da).[35,36]

Interestingly, the tandem reaction was found to occur in *E. coli*. Thus, incubating cells with **RuSCNP** and βGal, rinsing to remove free enzyme and nanoparticle, followed by incubation with **8** and irradiation led to an increase in fluorescence as determined using flow-cytometry (Figure 4d). Increasing irradiation times gave increased fluorescence whereas control experiments lacking substrate **8**, **RuSCNP**, or irradiation showed negligible change in fluorescence.

Based on the interaction between **RuSCNP** and *E. coli* observed by flow-cytometry (Figure S10), two possible limiting models emerged. In the first, the dual catalysis occurs within the bacterial cells. There are scattered reports of nanoparticles and assemblies being internalized by *E. coli*,[37,38] this model involving cooperative uptake of βGal and **RuSCNP**. Alternatively, the βGal-**RuSCNP** complex might adhere to the surface[39] of the *E. coli* and the dual catalysis occurs extracellularly or within the cell membrane, the product then entering the cell. Because there are no extracellular reducing agents, this model would require some form of membrane disruption to allow activation of the $Ru(bpy)_3$.

Our previous work demonstrated that the SCNP scaffold can make a metallocatalyst function like an enzyme.[14,15] Here we demonstrated that this functionality can work in concert with enzymes to perform both concurrent and tandem catalysis in living cells. Importantly, a new role of the SCNP is established, that of a carrier to facilitate cellular uptake of an enzyme. In this instance, the **RuSCNP** complexes βGal and delivers it to endosomes. The nanoparticle and the enzyme both remain active, thereby engineering the endosome as an artificial organelle for intracellular catalysis. In a broad sense this capability provides access to an intracellular molecular factory where diffusion of small precursor substrates into the cell can lead to the manufacturing of complex synthetic products on demand.

Supplementary Material

Refer to Web version on PubMed Central for supplementary material.

ACKNOWLEDGMENT

This work was supported by the National Science Foundation (NSF CHE-1709718) and the National Institutes of Health (R01AR058361).

REFERENCES

1. Bai Y; Chen J; Zimmerman SC, Designed transition metal catalysts for intracellular organic synthesis. Chem. Soc. Rev 2018, 47, 1811–1821. [PubMed: 29367988]
2. Soldevila-Barreda JJ; Metzler-Nolte N, Intracellular Catalysis with Selected Metal Complexes and Metallic Nanoparticles: Advances toward the Development of Catalytic Metallodrugs. Chem. Rev 2019, 119, 829–869. [PubMed: 30618246]
3. Yang M; Li J; Chen PR, Transition metal-mediated bioorthogonal protein chemistry in living cells. Chem. Soc. Rev 2014, 43, 6511–6526. [PubMed: 24867400]
4. Vidal C; Tomás-Gamasa M; Destito P; López F; Mascareñas JL, Concurrent and orthogonal gold(I) and ruthenium(II) catalysis inside living cells. Nat. Commun 2018, 9, 1913. [PubMed: 29765051]
5. Clavadetscher J; Indrigo E; Chankeshwara SV; Lilienkampf A; Bradley M, In-Cell Dual Drug Synthesis by Cancer-Targeting Palladium Catalysts. Angew. Chem. Int. Ed 2017, 56, 6864–6868.
6. Rudroff F; Mihovilovic MD; Gröger H; Snajdrova R; Iding H; Bornscheuer UT, Opportunities and challenges for combining chemo- and biocatalysis. Nature Catal. 2018, 1, 12–22.
7. Litman ZC; Wang Y; Zhao H; Hartwig JF, Cooperative asymmetric reactions combining photocatalysis and enzymatic catalysis. Nature 2018, 560, 355–359. [PubMed: 30111790]
8. Elsabahy M; Wooley KL, Design of polymeric nanoparticles for biomedical delivery applications. Chem. Soc. Rev 2012, 41, 2545–2561. [PubMed: 22334259]
9. Rothfuss H; Knöfel ND; Roesky PW; Barner-Kowollik C, Single-Chain Nanoparticles as Catalytic Nanoreactors. J. Am. Chem. Soc 2018, 140, 5875–5881. [PubMed: 29630817]
10. Miller MA; Askevold B; Mikula H; Kohler RH; Pirovich D; Weissleder R, Nano-palladium is a cellular catalyst for in vivo chemistry. Nat. Commun 2017, 8, 15906. [PubMed: 28699627]
11. Wang ZJ; Clary KN; Bergman RG; Raymond KN; Toste FD, A supramolecular approach to combining enzymatic and transition metal catalysis. Nat. Chem 2013, 5, 100. [PubMed: 23344446]
12. Rebelein JG; Ward TR, In vivo catalyzed new-to-nature reactions. Curr. Opin. Biotechnol 2018, 53, 106–114. [PubMed: 29306675]
13. Cortes-Clerget M; Akporji N; Zhou J; Gao F; Guo P; Parmentier M; Gallou F; Berthon J-Y; Lipshutz BH, Bridging the gap between transition metal- and bio-catalysis via aqueous micellar catalysis. Nat. Commun 2019, 10, 2169. [PubMed: 31092815]
14. Chen J; Wang J; Bai Y; Li K; Garcia ES; Ferguson AL; Zimmerman SC, Enzyme-like Click Catalysis by a Copper-Containing Single-Chain Nanoparticle. J. Am. Chem. Soc 2018, 140, 13695–13702. [PubMed: 30192530]
15. Chen J; Wang J; Li K; Wang Y; Gruebele M; Ferguson AL; Zimmerman SC, Polymeric “Clickase” Accelerates the Copper Click Reaction of Small Molecules, Proteins, and Cells. J. Am. Chem. Soc 2019, 141, 9693–9700. [PubMed: 31124359]
16. Huerta E; Stals PJM; Meijer EW; Palmans ARA, Consequences of Folding a Water-Soluble Polymer Around an Organocatalyst. Angew. Chem. Int. Ed 2013, 52, 2906–2910.
17. Liu Y; Turunen P; de Waal BFM; Blank KG; Rowan AE; Palmans ARA; Meijer EW, Catalytic single-chain polymeric nanoparticles at work: from ensemble towards single-particle kinetics. Mol. Syst. Des. Eng 2018, 3, 609–618.
18. Rubio-Cervilla J; González E; Pomposo J, Advances in Single-Chain Nanoparticles for Catalysis Applications. Nanomaterials 2017, 7, 341–360. [PubMed: 29065489]
19. Cole JP; Hanlon AM; Rodriguez KJ; Berda EB, Protein-like structure and activity in synthetic polymers. J. Polym. Sci. Pol.Chem 2017, 55, 191–206.
20. Pomposo JA, Ed. Single-Chain Polymer Nanoparticles: Synthesis, Characterization, Simulations, and Applications; John Wiley & Sons, 2017.

21. Bai Y; Xing H; Wu P; Feng X; Hwang K; Lee JM; Phang XY; Lu Y; Zimmerman SC, Chemical Control over Cellular Uptake of Organic Nanoparticles by Fine Tuning Surface Functional Groups. ACS Nano 2015, 9, 10227–10236. [PubMed: 26327513]
22. Bai Y; Feng X; Xing H; Xu Y; Kim BK; Baig N; Zhou T; Gewirth AA; Lu Y; Oldfield E; Zimmerman SC, A Highly Efficient Single-Chain Metal–Organic Nanoparticle Catalyst for Alkyne–Azide "Click" Reactions in Water and in Cells. J. Am. Chem. Soc 2016, 138, 11077–11080. [PubMed: 27529791]
23. Liu Y; Pujals S; Stals PJM; Paulöhrl T; Presolski SI; Meijer EW; Albertazzi L; Palmans ARA, Catalytically Active Single-Chain Polymeric Nanoparticles: Exploring Their Functions in Complex Biological Media. J. Am. Chem. Soc 2018, 140, 3423–3433. [PubMed: 29457449]
24. Chen Y; Kamlet AS; Steinman JB; Liu DR, A biomolecule-compatible visible-light-induced azide reduction from a DNA-encoded reaction-discovery system. Nat. Chem 2011, 3, 146. [PubMed: 21258388]
25. Angerani S; Winssinger N, Visible Light Photoredox Catalysis Using Ruthenium Complexes in Chemical Biology. Chem. Eu. J 2019, 25, 6661–6672.
26. Sadhu KK; Eierhoff T; Römer W; Winssinger N, Photoreductive Uncaging of Fluorophore in Response to Protein Oligomers by Templated Reaction in Vitro and in Cellulo. J. Am. Chem. Soc 2012, 134, 20013–20016. [PubMed: 23186060]
27. Holtzer L; Oleinich I; Anzola M; Lindberg E; Sadhu KK; Gonzalez-Gaitan M; Winssinger N, Nucleic Acid Templated Chemical Reaction in a Live Vertebrate. ACS Cent. Sci 2016, 2, 394–400. [PubMed: 27413783]
28. Sasmal PK; Carregal-Romero S; Han AA; Streu CN; Lin Z; Namikawa K; Elliott SL; Köster RW; Parak WJ; Meggers E, Catalytic Azide Reduction in Biological Environments. ChemBioChem 2012, 13, 1116–1120. [PubMed: 22514188]
29. Hsu H-T; Trantow BM; Waymouth RM; Wender PA, Bioorthogonal Catalysis: A General Method To Evaluate Metal-Catalyzed Reactions in Real Time in Living Systems Using a Cellular Luciferase Reporter System. Bioconjug. Chem 2016, 27, 376–382. [PubMed: 26367192]
30. Ghosh P; Yang X; Arvizo R; Zhu Z-J; Agasti SS; Mo Z; Rotello VM, Intracellular Delivery of a Membrane-Impermeable Enzyme in Active Form Using Functionalized Gold Nanoparticles. J. Am. Chem. Soc 2010, 132, 2642–2645. [PubMed: 20131834]
31. Berg JD; Fiksdal L, Rapid detection of total and fecal coliforms in water by enzymatic hydrolysis of 4-methylumbelliferone-beta-D-galactoside. Appl. Environ. Microbiol 1988, 54, 2118–2122. [PubMed: 3178215]
32. Brakel R. v.; Vulders RCM; Bokdam RJ; Grüll H; Robillard MS, A Doxorubicin Prodrug Activated by the Staudinger Reaction. Bioconjug. Chem 2008, 19, 714–718. [PubMed: 18271515]
33. Doura T; Takahashi K; Ogra Y; Suzuki N, Combretastatin A4-β-Galactosyl Conjugates for Ovarian Cancer Prodrug Monotherapy. ACS Med. Chem. Lett 2017, 8, 211–214. [PubMed: 28197314]
34. Wang R; Cai K; Wang H; Yin C; Cheng J, A caged metabolic precursor for DT-diaphorase-responsive cell labeling. Chem. Commun 2018, 54, 4878–4881.
35. Lipinski CA; Lombardo F; Dominy BW; Feeney PJ, Experimental and computational approaches to estimate solubility and permeability in drug discovery and development settings. Adv. Drug Deliv. Rev 1997, 23, 3–25.
36. Lee J; Bai Y; Chembazhi UV; Peng S; Yum K; Luu LM; Hagler LD; Serrano JF; Chan HYE; Kalsotra A; Zimmerman SC, Intrinsically cell-penetrating multivalent and multitargeting ligands for myotonic dystrophy type 1. Proc. Natl. Acad. Sci 2019, 116, 8709–8714. [PubMed: 30975744]
37. Kumar M; Tegge W; Wangoo N; Jain R; Sharma RK, Insights into cell penetrating peptide conjugated gold nanoparticles for internalization into bacterial cells. Biophys. Chem 2018, 237, 38–46. [PubMed: 29656216]
38. Jiao J-B; Wang G-Z; Hu X-L; Zang Y; Maisonneuve S; Sedgwick AC; Sessler JL; Xie J; Li J; He X-P; Tian H, Cyclodextrin-Based Peptide Self-Assemblies (Spds) That Enhance Peptide-Based Fluorescence Imaging and Antimicrobial Efficacy. J. Am. Chem. Soc 2020, 142, 1925–1932. [PubMed: 31884796]

39. Hayden SC; Zhao GX; Saha K; Phillips RL; Li XN; Miranda OR; Rotello VM; El-Sayed MA; Schmidt-Krey I; Bunz UHF, Aggregation and Interaction of Cationic Nanoparticles on Bacterial Surfaces. J. Am. Chem. Soc 2012, 134, 6920–6923. [PubMed: 22489570]

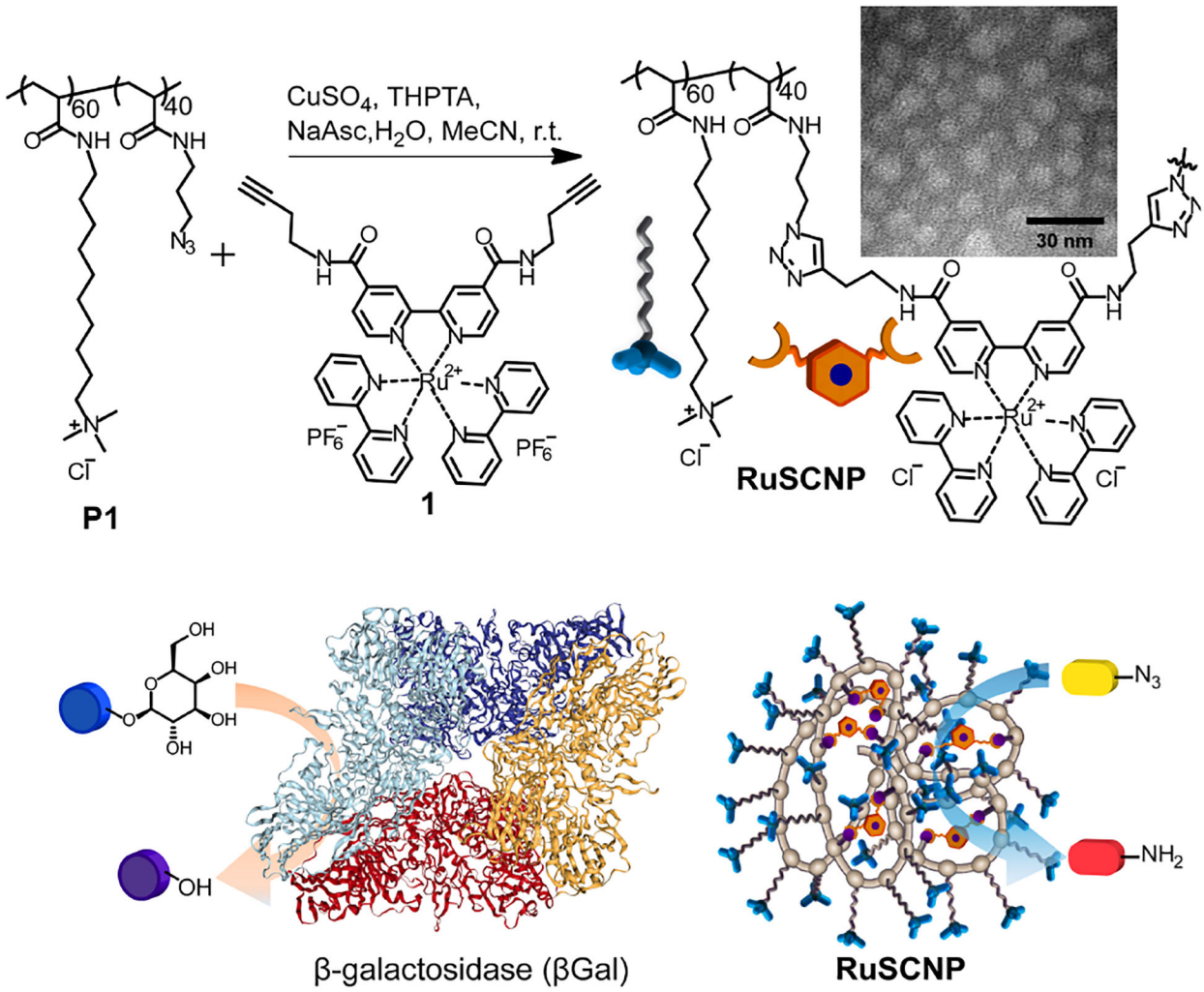

Figure 1.
Illustration of **RuSCNP** preparation and dual catalysis with βGal.

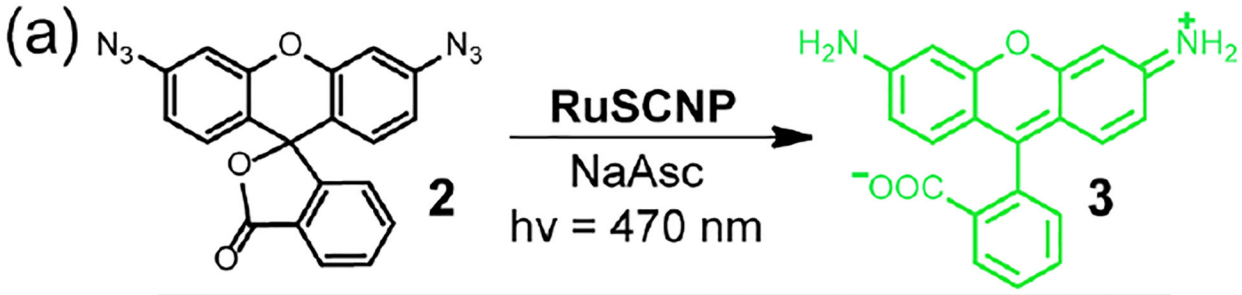

Conversion	RuSCNP	1	Ru(bpy)$_3$
2 min	43%	5%	4%
5 min	78%	27%	15%
10 min	>97%	52%	23%

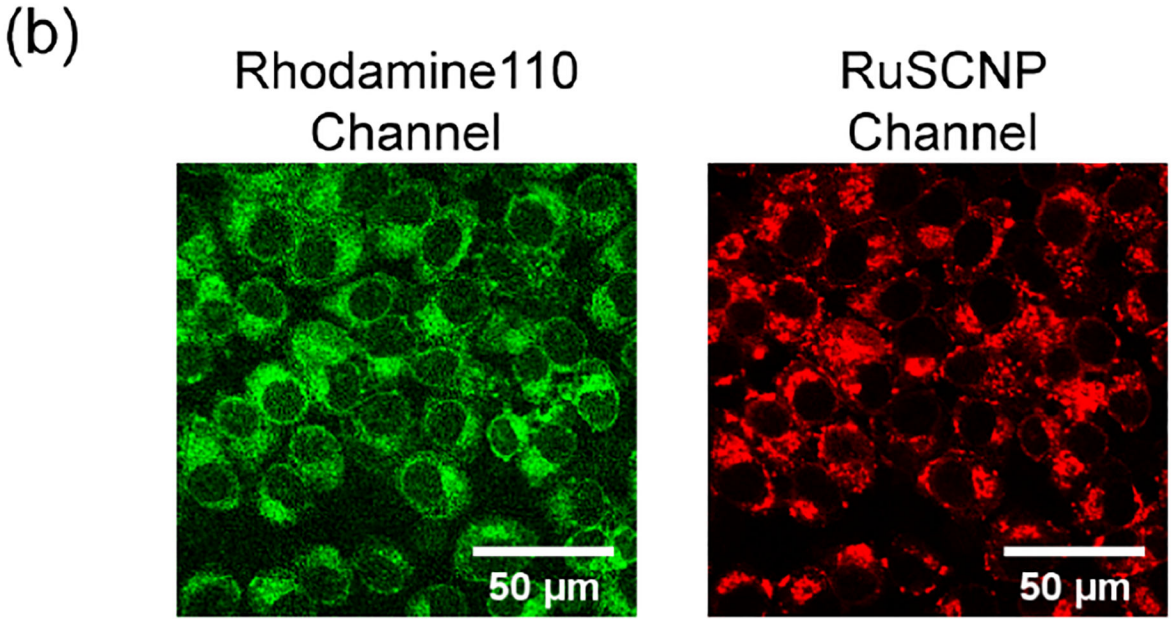

Figure 2.

RuSCNP mediated azide reduction. (a) Fluorogenic reactions at room temperature with **2** (5 μM), NaAsc (2 mM) and catalyst. [**RuSCNP**] = 50 nM, [**1**] = 1 μM, [Ru(bpy)$_3$] = 1 μM. (b) Confocal images of HeLa cells after 5 min irradiation at 470 nm. Cells were treated with **RuSCNP** (200 nM) and **2** (20 μM) for 4 h.

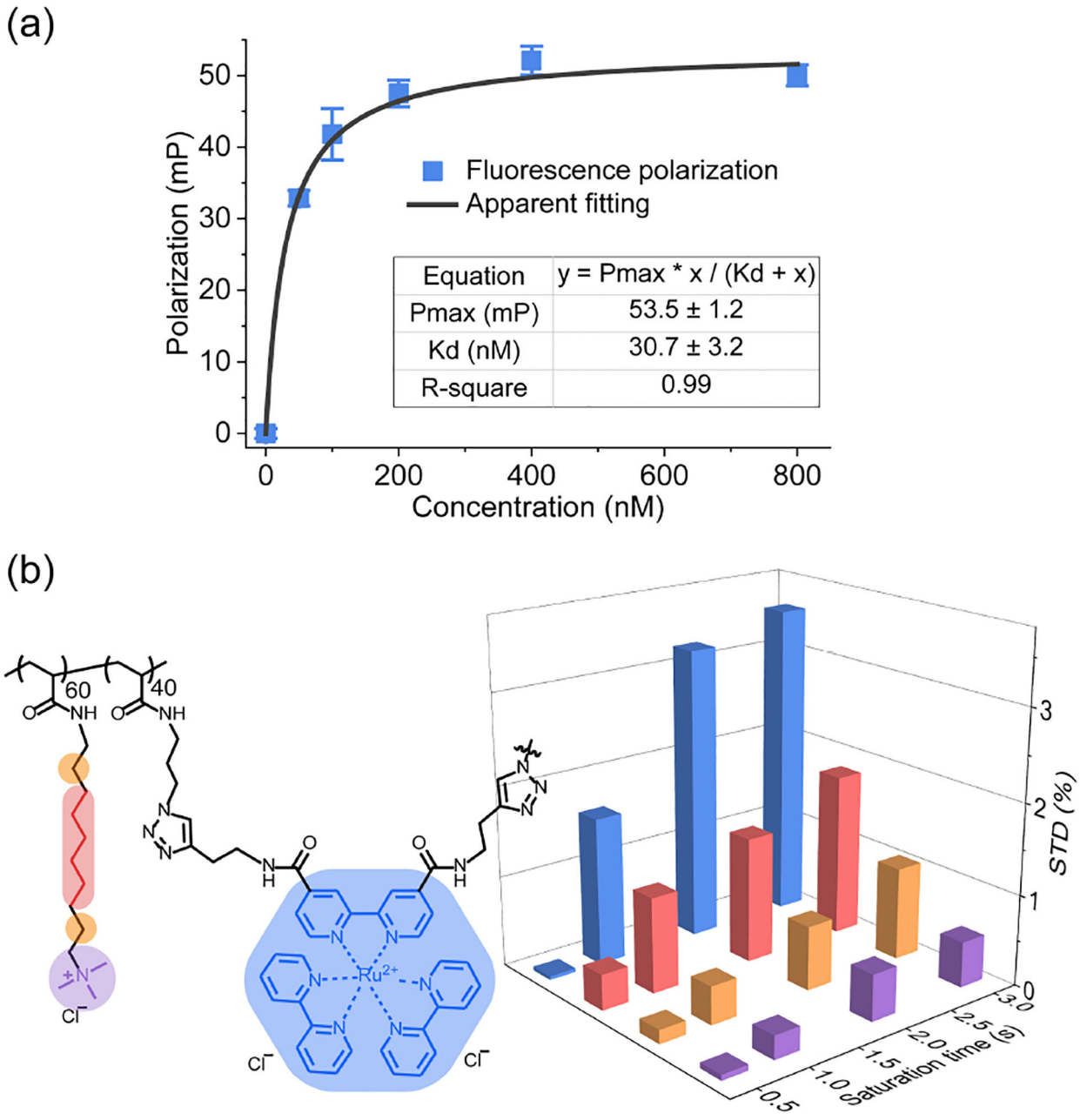

Figure 3.

SCNP-enzyme binding study. (a) Fluorescence polarization of βGalF (20 nM) with different concentration of **RuSCNP** in PBS buffer. Error bars represent standard deviation of three runs. (b) Percentage of STD signals of **RuSCNP** (50 μM) with βGal (5 μM) in deuterium PBS buffer irradiated at −0.5 ppm for different saturation times.

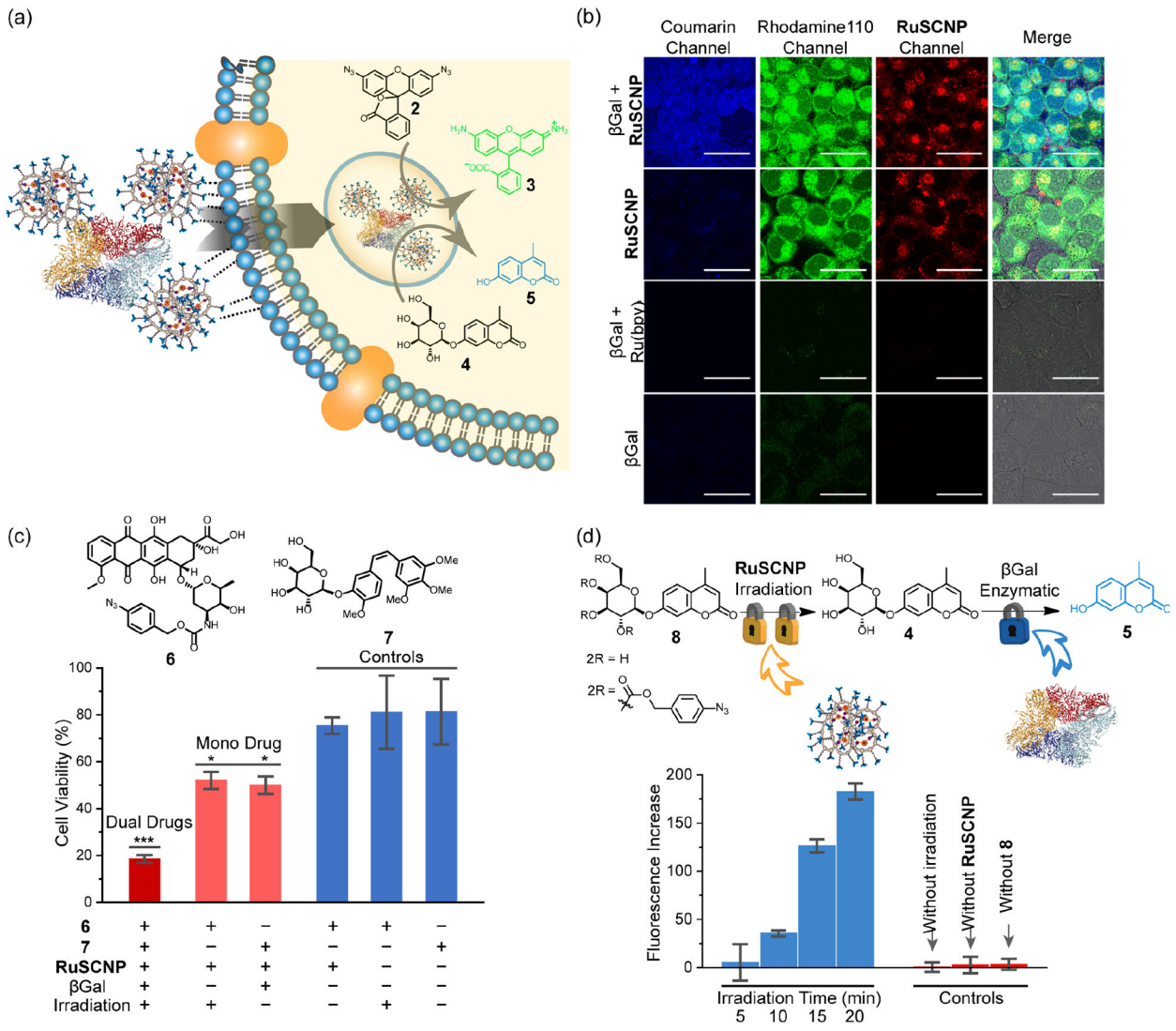

Figure 4.

Intracellular dual catalysis. (a) Illustration of SCNP-enzyme co-delivery and dual catalysis. (b) Confocal images of HeLa cells after 10 min irradiation at 470 nm. Cells treated with **2** (20 μM), **3** (100 μM), [βGal] = 20 nM, and catalyst, either [**RuSCNP**] = 200 nM or [$Ru(bpy)_3$] = 4 μM for 4h. (c) Intracellular dual drug activation. Cell viability of HeLa cells measured by MTT assay after experiments conducted with/without **6** (1 μM), **7** (4 μM), **RuSCNP** (200 nM), βGal (20 nM) and 5 min irradiation at 470 min. Error bars are standard deviation of three independent runs. *P ≤ 0.05, ***P ≤ 0.001. (d) Illustration of SCNP-enzyme tandem reaction conducted with **RuSCNP** and βGal. Flow-cytometry analysis of *E. coli* cells conducted with/without **8** (20 μM), **RuSCNP** (200 nM), βGal (20 nM) and irradiation. Error bars are standard error of three independent runs.